Clay Intercalation of Poly(styrene−ethylene oxide) Block Copolymers Studied by Two-Dimensional Solid-State NMR

S.-S. Hou,[†] T. J. Bonagamba,[†,‡] F. L. Beyer,[§] P. H. Madison,[§] and K. Schmidt-Rohr*[,†]

Ames Laboratory and Department of Chemistry, Iowa State University, Ames, Iowa 50011; Instituto de Física de São Carlos, Universidade de São Paulo, Caixa Postal 369, CEP: 13560-970, São Carlos-SP, Brazil; and US Army Research Laboratory, Polymers Research Branch, Bldg. 4600, Aberdeen Proving Grounds, Maryland 21005

Received October 2, 2002; Revised Manuscript Received February 19, 2003

ABSTRACT: The intercalation of poly(styrene−ethylene oxide) block copolymers (PS-*b*-PEO) into a smectite clay, hectorite, has been studied by multinuclear solid-state nuclear magnetic resonance (NMR). The behaviors of two copolymers with similar PEO block lengths (7 and 8.4 kDa) but different PS block lengths (3.6 vs 30 kDa) were compared. Polymer intercalation is assessed by two-dimensional $^{1}H-^{29}Si$ heteronuclear correlation (HETCOR) NMR with spin diffusion and refocused ^{29}Si detection for enhanced sensitivity. Hydroxyl protons in the smectite layers serve as crucial spin diffusion references and ^{1}H magnetization relay points from the polymer to the ^{29}Si in the silicate. Experiments with CRAMPS evolution, with ^{1}H spin diffusion, and with detection of the sharp OH proton signal after a ^{1}H T_2 filter provide excellent sensitivity for spin diffusion studies with mixing-time series. Because of the mobility of PEO, in this homonuclear experiment we can observe PEO−PS and clay−polymer spin diffusion simultaneously. While the PS block is found not to be intercalated in either copolymer, definite proof of PEO intercalation in the sample with the shorter, 3.6 kDa PS block is provided by a $^{1}H-^{13}C$ HETCOR spectrum. In the PS-rich sample, the amount of intercalated PEO is much smaller, and a significant fraction of PEO is not intercalated. Two-dimensional $^{1}H-^{29}Si$ correlation NMR without ^{1}H homonuclear decoupling shows that intercalated PEO has a clearly reduced mobility, most prominently for the PEO nearest to the silicate surface. A model of the PEO blocks intercalating sideways into 50 nm diameter stacks of hectorite can explain the experimental results.

Introduction

Nanocomposites of organic polymers with layered smectite clay minerals, such as montmorillonite or hectorite, have received significant interest in the past few years because of potentially strong synergistic effects between polymer and silicate layers.[1−4] This may result in improvements in mechanical and thermal properties due to the large contact area between polymer and clay on a nanometer length scale.

Traditionally, organically modified clay with small-molecule surfactants such as onium salts has been needed for intercalation of hydrophobic guest polymer because hydrophilic characteristics on the silicate layer surface prevent intercalation. However, the effectiveness of such surfactants is limited by their length and by the enthalpic interaction between the surfactant and intercalating polymer. In this work, a potential alternative to this procedure is explored. Certain hydrophilic polymers such poly(ethylene oxide) (PEO) have been shown to easily intercalate into unmodified layered silicate.[5,6] Rather than displacing interlayer cations naturally found on the layer surface, PEO is thought to solvate the cations and form a predominantly helical structure within the silicate galleries.[7] For amphiphilic diblock copolymers of polystyrene (PS) and PEO, the ability of PEO to intercalate into the layered silicate galleries of unmodified clay might facilitate intercalation of PS. Analogous to the modification of layered silicate by small-molecule surfactants, the polar PEO block can be expected to be drawn to the silicate layer surface and into the silicate gallery. Fisher et al. had previously prepared nanocomposites of PS−PEO block copolymers with short PS and PEO block lengths (1−3 kDa) and characterized them by X-ray diffraction.[8] They reported that the nanocomposite, from the block copolymer with PEO length of 1 kDa and PS length of 3 kDa, was partially exfoliated due to the action of the longer PS blocks, since it showed a substantially smaller intensity of the (001) peak at $2\theta = 5°$. However, this interpretation is problematic, since layer disorder, silicate volume fractions, and experimental conditions will all affect the basal reflection patterns.[4,9] Therefore, the question remains: will hydrophilic PEO pull hydrophobic PS into the silicate galleries? This is difficult to answer by small-angle X-ray diffraction or transmission electron microscopy (TEM) alone because these methods cannot identify the chemical structure of the intercalated polymer in the silicate gallery.

Solid-state nuclear magnetic resonance (NMR) spectroscopy is an excellent method to provide information on the microstructure, mobility, and conformation of molecules as well as on the chemical composition in solid materials.[10] Multinuclear solid-state NMR spectroscopy has been applied to study nanostructures and dynamics of a few polymer−clay nanocomposites.[11−13] Although NMR studies have been hampered by paramagnetic Fe^{3+} in the common montmorillonite clay, this problem has been largely circumvented by studies using the related, less-paramagnetic hectorite which has the same crystal structure as montmorillonite clay. The major difference in chemical composition between these two clays is that the octahedral sites in montmorillonite are

[†] Iowa State University.
[‡] Universidade de São Paulo.
[§] US Army Research Laboratory.
* To whom correspondence should be addressed: Tel (515) 294-6105, Fax (515) 294-0105, e-mail srohr@iastate.edu.

10.1021/ma025707f CCC: $25.00
Published on Web 03/27/2003

Table 1. Compositions of the Clay Block Copolymer Nanocomposites and the Corresponding Silicate Interlayer Spacings

sample	clay	PS M_n[a]	PEO M_n[a]	PDI[b]	ϕ_{PEO}[c]	D (nm)[d]
PS30EO-HCT	HCT	29800	8400	1.03	0.197	1.48
PS4EO-HCT	HCT	3600	7000	1.05	0.628	1.92

[a] Number-average molecular weight of the component polymer. [b] Polydispersity index of the diblock copolymer. [c] Volume fraction of PEO, which was calculated assuming an average density of 1.05 g/cm^3 for PS and 1.21 g/cm^3 for PEO. [d] Interlayer spacing, determined by X-ray diffraction.

occupied by Al^{3+}, Mg^{2+}, and Fe^{3+}, while they are mostly Mg^{2+} and Li^+ in hectorite. In our previous technical study,[14] we have established multinuclear NMR approaches for characterizing clay−polymer nanocomposites with very good sensitivity and selectivity, achieved most importantly by high-sensitivity refocused ^{29}Si NMR detection. In this work, these NMR experiments, such as ^{1}H−^{29}Si heteronuclear correlation (HETCOR) and ^{1}H−^{1}H correlation with spin diffusion, ^{1}H−^{29}Si wide-line separation (WISE) with spin diffusion, and ^{1}H−^{13}C HETCOR, are successfully applied to elucidate, on the nanometer scale, the extent of intercalation and the microstructure of PS-*b*-PEO copolymers in hectorite clay.

Experimental Section

Samples. The Na^+−hectorite (HCT) was obtained from the Source Clay Minerals Repository, University of Missouri−Columbia. The pristine clay mineral was cleaned by dispersion in deionized water and centrifuged to separate the dispersed clay from impurities. Afterward, the clay was dried in an oven at 65 °C and then was heated to 80 °C under vacuum for several days. Polystyrene-*block*-poly(ethylene oxide) (PS-*b*-PEO) diblock copolymers with low polydispersity were obtained commercially (Polymer Source, Inc., Canada), and their molecular characteristics are listed in Table 1. In the following, the polymers will be designated as PS4EO and PS30EO based on the MW of the PS block, which is 3.6 and 29.8 kDa, respectively.

To prepare the clay-intercalated block copolymers, the clay was ground into a coarse powder using a mortar and pestle. Samples composed of approximately 4 parts clay to 1 part block copolymer were mixed. The mixtures were pressed into pellets and annealed under vacuum above 120 °C for a minimum of 40 h. The pellets were then ground into powder form for NMR experiments.

X-ray Diffraction. The interlayer spacing of intercalated HCT was analyzed by an X-ray powder diffractometer (Scintag Inc., USA, XDS 2000 using a Cu target at 40 kV and 30 mA).

Transmission Electron Microscopy. For transmission electron microscopy (TEM) analysis, the modified clay samples were compacted into a pellet along with high molecular weight (100 000 g/mol) polystyrene (PS), using a pellet press and minimal, contact pressure. The PS acts as a support for the modified clay but, because of the high molecular weight, does not interact with the clay itself. The samples were annealed overnight at 130 C and under vacuum to allow the PS support to coalesce into a bulk material. Thin sections of the resulting pellets were cut using a Leica UCT ultramicrotome and a Microstar diamond knife; the sections are approximately 700 Å thick. TEM was performed using a JEOL 200 CX (S)TEM operated at an accelerating voltage of 200 kV.

NMR Measurements. All NMR experiments were performed on a Bruker DSX-400 spectrometer at resonance frequencies of 400 MHz for ^{1}H, 100 MHz for ^{13}C, and 79.5 MHz for ^{29}Si, using a double-resonance magic-angle spinning (MAS) probe with 7 mm o.d. rotors. The MAS spinning speed was set at 5 or 5.5 kHz. Recycle delays of 1−2 s were used. The ^{1}H, ^{29}Si, and ^{13}C pulse lengths were ca. 4 μs. Two-pulse phase modulation (TPPM)[15] was used for ^{1}H−^{29}Si or ^{1}H−^{13}C heteronuclear dipolar decoupling. ^{1}H and ^{29}Si chemical shifts were referenced to the methyl protons of external ethanol, at 1.11 ppm, and the downfield ^{29}Si peak of external tetrakis(trimethylsilyl)silane, −9.8 ppm, with respect to tetramethylsilane (TMS),[16] respectively. All experiments were carried out at ambient temperature.

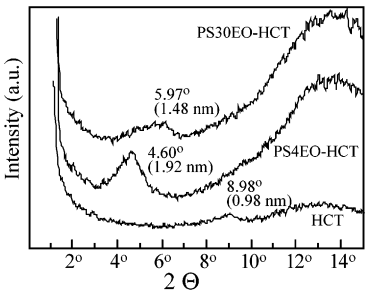

Figure 1. WAXD diffractograms of neat hectorite clay and of hectorite−copolymer nanocomposites, PS30EO-HCT and PS4EO-HCT. The diffractograms were plotted on the same *Y*-axis scale but were displaced vertically in order to display the individual diffractogram more clearly.

In all 2D ^{1}H−^{29}Si HETCOR experiments, ca. 5-fold ^{29}Si signal enhancement was achieved by refocusing the ^{29}Si magnetization using multiple Hahn echoes that stretch the signal of ^{29}Si from $T_2^* = 1.5$ ms to $T_2 = 80$ ms.[14] A magic-angle spin lock was used to avoid ^{1}H spin diffusion during ^{1}H−^{29}Si cross-polarization (Lee−Goldburg cross-polarization, LGCP).[14] For each 2D ^{1}H−^{29}Si HETCOR spectrum of the PS4EO-HCT sample, 192 slices were acquired in the t_1 dimension and the number of scans was 16; the measuring time was 2 h. For each 2D ^{1}H−^{1}H correlation spectrum, 200 slices were acquired in the t_1 dimension and the number of scans was 16 per t_1 slice; the measuring time was 100 min per spectrum. For the 2D ^{1}H−^{13}C HETCOR spectrum, 32 slices were acquired in the t_1 dimension and the number of scans was 1024; the measuring time was 12 h. The technical details of the pulse sequences and parameters for the two-dimensional NMR experiments used in this work, as well as experiments for clay-OH signal[17] assignment, have been described in a separate study.[14]

Results and Discussion

X-ray Diffraction. Figure 1 shows the wide-angle X-ray diffraction (WAXD) patterns of pure hectorite clay (HCT) and of two clay/copolymer nanocomposites. The shift in the position of the interlayer reflection indicates an increase in the intersilicate gallery height from that in the original HCT by ca. 0.5 nm for PS30EO-HCT and 1 nm for PS4EO-HCT. The diffraction peak for PS4EO-HCT is more obvious and sharper than that of PS30EO-HCT, indicating a more ordered intercalated structure. However, the details of the structural organization of the polymer blocks with respect to the clay are not clear from the diffraction data alone. For instance, the gallery height found in PS4EO-HCT is larger than that of either of the two stable complexes of PEO homopolymer with hectorite clay.[7] Therefore, we have characterized these systems in more detail by solid-state NMR.

Transmission Electron Microscopy. TEM is an excellent qualitative method to characterize intercalated and exfoliated nanostructures of polymer−clay nanocomposites. The WAXD patterns indicate that the intercalated nanostructures of PS4EO-HCT and PS30EO-HCT are quite different. However, in Figure 2 the TEM images of PS4EO-HCT and PS30EO-HCT look largely alike, and no significant difference in interlayer spacing between the two samples is detectable. Unlike NMR, TEM cannot easily identify the chemical structure of the intercalated polymer.

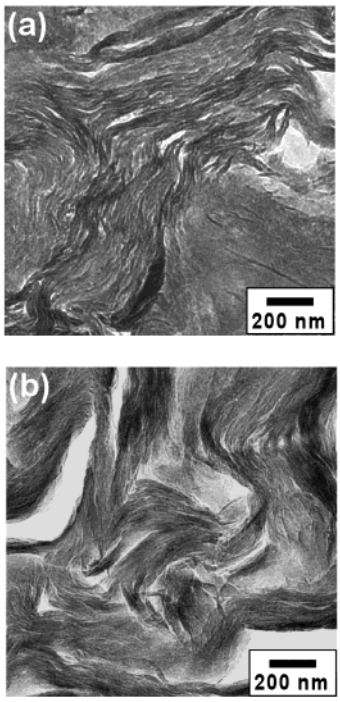

Figure 2. Transmission electron micrographs of (a) PS4EO-HCT and (b) PS30EO-HCT. The two samples look largely alike, and no significant difference in interlayer spacing is discernible.

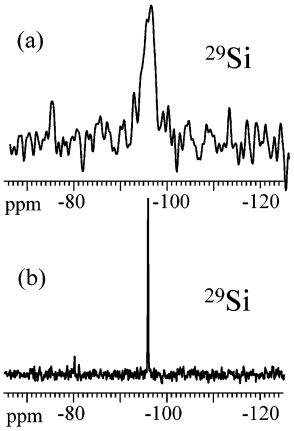

Figure 3. (a) Cross-polarized ^{29}Si spectrum of hectorite in the PS30EO-HCT sample. Since all silicon sites are equivalent (Q^3 environment), only one resonance line is observed. (b) Fivefold signal-to-noise enhancement by multiple Hahn-echo refocusing. Spinning frequency: 5 kHz. Number of scans: 16. ^{1}H−^{29}Si Lee−Goldburg cross-polarization (LGCP) time: 1.5 ms.

^{29}Si NMR with High-Sensitivity Si Detection. For systematic ^{29}Si NMR studies of clay−polymer nanocomposites, high sensitivity is required. We have found[14] that the sensitivity of the ^{29}Si signal can be enhanced 5-fold by multiple Hahn-echo refocusing of the ^{29}Si magnetization during the period of detection, as demonstrated in ^{29}Si CP/MAS NMR spectra of PS30EO-HCT shown in Figure 3. The single ^{29}Si resonance peak at −96 ppm in Figure 3a indicates that all silicon sites in the hectorite clay have the same Q^3 environment.[18,19] Figure 3b shows the corresponding ^{29}Si spectrum obtained by refocused on-resonance detection at the same numbers of scans; a very sharp ^{29}Si signal with good signal-to-noise ratio is clearly visible. Since the information of interest in the following ^{1}H−^{29}Si HETCOR and WISE experiments is contained in the modulation of the ^{29}Si signal due to the evolution of the ^{1}H magnetization before cross-polarization, the loss in ^{29}Si chemical shift information resulting from the refocusing is of little consequence.

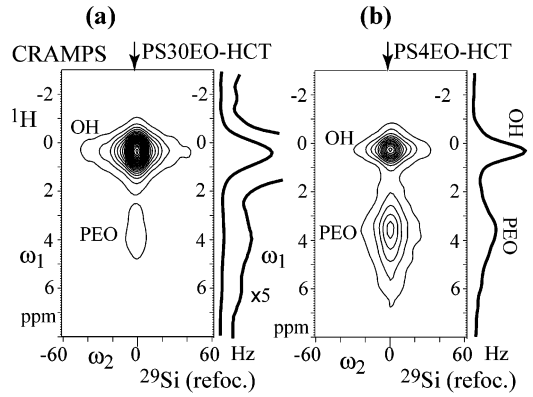

Figure 4. Two-dimensional ^{1}H−^{29}Si HETCOR spectrum with 1 ms of ^{1}H spin diffusion before CP for (a) PS30EO-HCT and (b) PS4EO-HCT, at $\nu_r = 5$ kHz. The homonuclear decoupled (FSLG) ^{1}H spectrum along the ω_1 dimension, taken at the center of the Si signal as marked by the arrows, is shown to the right of the 2D spectrum. ^{1}H−^{29}Si LGCP time: 1.5 ms.

^{1}H−^{29}Si HETCOR with Spin Diffusion. Figure 4 shows the ^{1}H−^{29}Si correlation spectra of PS30EO-HCT and PS4EO-HCT at a spin diffusion mixing time of 1 ms, with high-sensitivity refocused ^{29}Si detection.[14] The proton spectrum shown at the right of each spectrum, obtained in the ω_1 dimension under multiple-pulse homonuclear decoupling (CRAMPS),[20] reflects the ^{1}H chemical shifts of organic moieties near the clay surface. The cross-peak at 0.35 ppm in the ω_1 dimension shown in Figure 4 was assigned to the clay-OH protons of silicate in our previous study, and the Si−H internuclear distance was determined as 2.9 ± 0.4 Å in a ^{1}H−^{29}Si REDOR experiment on pure hectorite.[14] As a consequence, the spectrum in the ω_1 dimension represents the protons whose magnetization diffuses, within 1 ms, to the OH protons that cross-polarize the ^{29}Si nuclei. They reside in polymer segments at 0.3−2 nm distances from the surface of silicate. The PEO signal visible in the spectrum of Figure 4b indicates that the PEO blocks of PS4EO do intercalate significantly into the silicate galleries. The extent of intercalation of PS-*b*-PEO copolymers can thus be assessed by ^{1}H−^{29}Si HETCOR with spin diffusion, whose duration can be varied.

Figure 5 shows cross sections at the center of the ^{29}Si peak in the ω_2 dimension, obtained from a mixing time series of ^{1}H−^{29}Si 2D spectra with refocused ^{29}Si detection. For the PS4EO-HCT sample, at short mixing times ($t_m = 0$, 0.3, and 1 ms in Figure 5a), the cross sections reveal a small, but clear, PEO proton peak, indicating that the PEO block of PS4EO copolymer is in close contact with the silicate surface. Within 3 ms of spin diffusion, the intensity of the OH proton peak has decreased significantly, and the PEO proton peak has become dominant in the spectra. This fast spin diffusion between PEO and OH protons must be the result of intercalation of the PEO segments into the silicate gap. At long times, $t_m = 100$ ms, a faint shoulder at the 7 ppm PS band position becomes visible.

In contrast, for PS30EO-HCT (Figure 5b) a significant PEO or H_2O proton peak near 4 ppm appears only after a mixing time of 10 ms, indicating a much smaller amount of intercalated PEO. All 2D ^{1}H−^{29}Si HETCOR

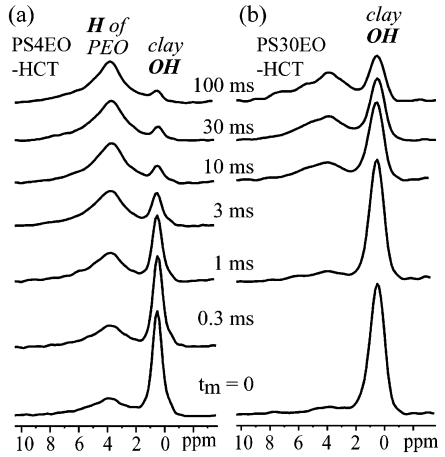

Figure 5. Cross sections taken at the center of the Si peak in 2D $^1H-^{29}Si$ HETCOR spectra for a series of spin diffusion mixing times. (a) PS4EO-HCT; (b) PS30EO-HCT. The data in (a) show fast spin diffusion from PEO protons, while those in (b) exhibit little evidence of polymer intercalation. The spectra in each series have been scaled to equal area, which reduces the effect of ^1H T_1 relaxation. LGCP time: 1.5 ms.

spectra of these two samples do not show any significant cross-peak between Si and the PS protons, expected near 7 ppm, within mixing times of less than 30 ms. This shows clearly that the PS block is not intercalated. All spectra in this figure have been corrected for ^1H T_1 relaxation. The relaxation is nonexponential, but it can be roughly characterized by the time of decay to 0.61, which is 100 ms for PS4EO-HCT and 35 ms for PS30EO-HCT. We have found very short ^1H T_1 relaxation times to be indicative of intercalated H_2O. For instance, in hydrated hectorite the ^1H T_1 of H_2O is less than 5 ms. As a result, H_2O protons are almost invisible in these spin diffusion experiments.

$^1H-^{13}C$ "HETCOR" with Spin Diffusion. Further evidence of intercalation of the PS4EO block copolymer can be offered by $^1H-^{13}C$ correlation NMR with spin diffusion before CP. The goal is the correlation of the silicate OH proton signal with the ^{13}C resonances of the intercalated polymer. This identifies intercalated species clearly in terms of their ^{13}C NMR spectrum. In particular, this provides an unambiguous distinction of PEO and H_2O signals. In contrast to standard solid-state HETCOR NMR, no homonuclear decoupling is required during ^1H evolution. The OH signal is narrowed sufficiently by MAS alone.[14] In addition, this approach avoids overlap of the OH signal of interest with rigid-polymer proton signals, which dephase fast in the time domain. In the spectrum, the rigid-polymer signals produce only a constant background in the ω_1 dimension, which was removed by a constant-baseline correction in the 2D spectrum.[14] Figure 6a shows the $^1H-^{13}C$ correlation NMR spectrum of PS4EO-HCT after 30 ms of ^1H spin diffusion. The cross section in Figure 6b, taken at the clay-OH proton resonance position in the ω_1 dimension, consists of a single peak at 70 ppm. This represents the ^{13}C spectrum of the intercalated PEO block; no signal of intercalated PS is detected.

For comparison, Figure 6c shows the cross section taken along the ^{13}C dimension ω_2 at the PEO-proton ω_1 peak position. Showing strong signals of both the PEO and PS blocks, it resembles the ^{13}C spectrum of the diblock copolymer. This shows that spin diffusion between the aromatic and aliphatic groups of PS and the protons of PEO has occurred within 30 ms. The

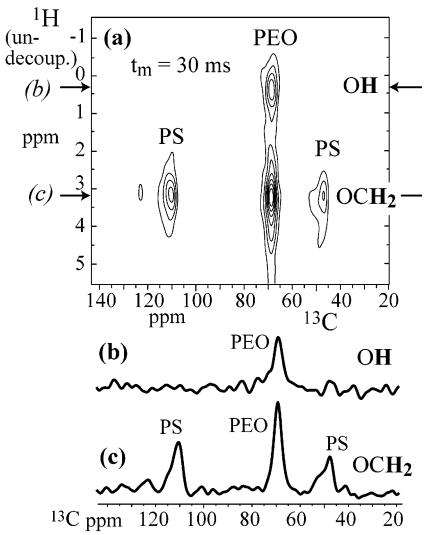

Figure 6. $^1H-^{13}C$ HETCOR NMR spectrum for PS4EO-HCT with 30 ms spin diffusion mixing time. Regular Hartmann–Hahn cross-polarization was used, with a relatively short duration of 150 μs in order to minimize signal loss from $T_{1\rho}$ relaxation. (a) 2D correlation spectrum. (b) Cross section at the clay-OH proton peak, representing the ^{13}C spectrum of polymer segments near the silicate surface, within the range of 30 ms of spin diffusion. No signals of intercalated PS are observed. (c) Cross section at the PEO proton peak, showing spin diffusion between the PEO and PS blocks.

absence of the cross-peaks between the PS block and the clay-OH protons in Figure 6a,b confirms conclusively that the PS block of the PS-*b*-PEO copolymer does not intercalate into the silicate galleries.

$^1H-^1H$ Correlation with Spin Diffusion. The OH proton signal at 0.35 ppm has a long T_2 relaxation time at sufficiently high spinning frequencies (>4 kHz) due to the large $^1H-^1H$ distances in the silicate.[14] Therefore, this signal can be selected by T_2-filtered detection in the ω_2 dimension of a 2D homonuclear correlation experiment with spin diffusion. In the first dimension, the ^1H spectrum of all the protons within spin diffusion range from the OH sites is recorded under multiple-pulse decoupling (CRAMPS). Such an experiment yields spectra very similar to 2D $^1H-^{29}Si$ HETCOR, but with higher sensitivity. Figure 7 demonstrates that the narrow clay OH signal is selected by the T_2-filtered detection. In addition, the signal of mobile PEO, which also has a long T_2, is observed. It is worth noting that the line of PEO in PS4EO-HCT is broader than that in PS30EO-HCT. This is an indication that the intercalated PEO segments in PS4EO-HCT are less mobile than those of the less constrained PEO in PS30EO-HCT (see below).

The proton spectrum of the polymer segments within a distance of several nanometers from the center of the silicate clay can be obtained by taking the cross section at the OH peak position in ω_2, as shown in Figure 8a for PS4EO-HCT and in Figure 8c for PS30EO-HCT. The PEO proton peak at 3.5 ppm in Figure 8a can be attributed to the intercalated PEO of the PS4EO copolymer. Its relatively large line width of 0.92 kHz is characteristic of intercalated PEO.[14] The lack of PS signal at mixing times <10 ms proves again that the PS block of the PS4EO copolymer is not intercalated. The aromatic-proton shoulder becoming visible at 100 ms reflects spin diffusion over ~10 nm between OH and PS protons, but equilibrium is not reached on this time

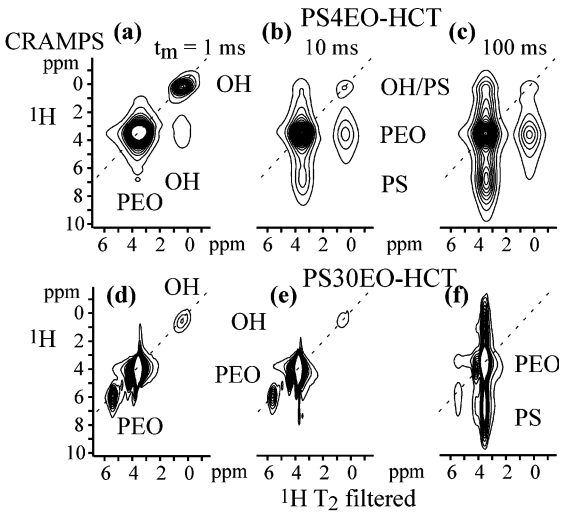

Figure 7. Two-dimensional ^{1}H−^{1}H correlation spectra for three mixing times for both samples: (a), (b), and (c) for PS4EO-HCT at t_m = 1, 10, and 100 ms, respectively. (d), (e), and (f) for PS30EO-HCT at t_m = 1, 10, and 100 ms, respectively. In the ω_2 dimension of each spectrum, a −300 Hz resolution enhancement was applied. The diagonals of the spectra are indicated as dashed lines.

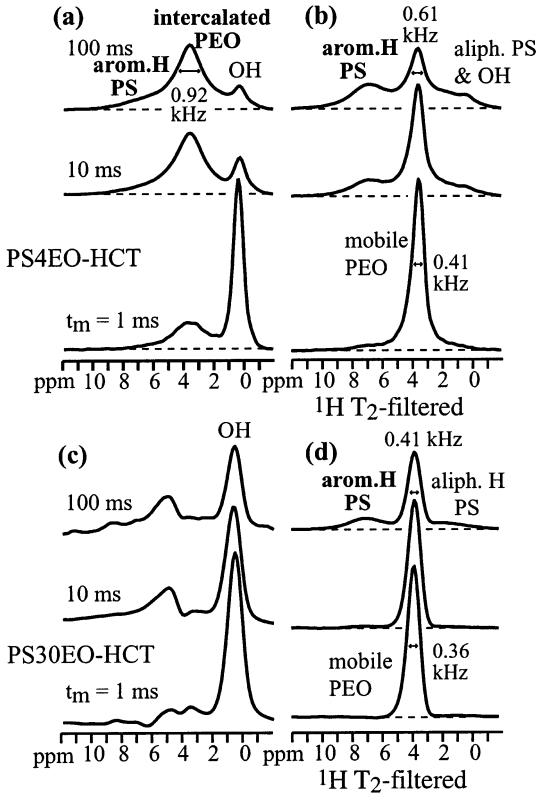

Figure 8. Spin diffusion series from ^{1}H−^{1}H correlation NMR: Cross sections of the spectra in Figure 6 at (a) the OH peak of PS4EO, (b) the PEO peak of PS4EO, (c) the OH peak of PS30EO, and (d) the PEO peak of PS30EO. The spectra agree closely with those of Figure 5.

scale. In the PS30EO-HCT sample, spin diffusion is again limited and quite slow.

Figure 8b,d shows a series of cross sections taken at the PEO peak position in ω_2, from the 2D spectra of Figure 7. For the PS4EO-HCT sample, the spectrum at the bottom of Figure 8b, which is the cross section taken at the position of the PEO proton signal for a 1 ms mixing time, exhibits a PEO proton peak with smaller line width (0.41 kHz), compared to those in Figure 8a. There is no PS or clay-OH signal visible in the spectrum of t_m = 1 ms, so this sharp PEO proton peak represents the protons of mobile PEO segments that are not intercalated. When the mixing time is longer, t_m = 10 and 100 ms, the clay-OH peak and PS aliphatic signals at <2 ppm and the PS aromatic peak at ca. 7 ppm appear, indicating spin diffusion between PS and PEO. In addition, the PEO proton peak along ω_1 becomes broader. This is apparently a consequence of diffusion of magnetization from the intercalated PEO segments to the detected mobile PEO protons. Assuming an effective spin diffusion coefficient of approximately 0.3 nm^2/ms for mobile PEO protons,[21] we can estimate that a ∼5 nm length of the PEO block connected to the PS block in PS4EO copolymer is not intercalated.

The spectra in Figure 8d are cross sections at the PEO proton signal position for the PS30EO-HCT sample. In the spectrum of t_m = 1 ms, similar to the PS4EO-HCT sample, the sharp PEO proton peak with line width of 0.36 kHz represents protons of mobile PEO segments that are not intercalated. At a mixing time of 100 ms, diffusion of magnetization between PS and PEO protons is observed, but the line width of the PEO proton peak is still as narrow as 0.41 kHz and no clay-OH peak shows up in the spectrum. This suggests that a significant fraction of the PEO block in the PS30EO copolymer is not intercalated.

^{1}H−^{29}Si "WISE" with Spin Diffusion. The mobility of the intercalated polymer can be assessed from its ^{1}H line width measured without homonuclear proton decoupling.[12] This is achieved in a wide-line-separation (WISE) experiment[22] with refocused ^{29}Si detection. Figure 9a,b shows the 2D WISE spectra for PS4EO-HCT for mixing times of 1 and 10 ms. In such spectra, only mobile polymer segments are detected with a narrow line because the dipolar coupling in rigid segments broadens the ^{1}H line by tens of kilohertz. The fraction of immobile segments can be estimated by comparing the WISE spectrum with the regular ^{1}H−^{29}Si HETCOR spectrum at the same spin diffusion time, which exhibits ^{1}H signals of all segments reached by spin diffusion regardless of their mobility.

In Figure 9, the polymer signals detected after a short spin diffusion time of 1 ms originate from the segments near the surface, whereas at long spin diffusion time (10 ms) more remote polymer segments are detected. After 1 ms of spin diffusion, the ^{29}Si−^{1}H HETCOR NMR spectrum (Figure 9e) shows a strong peak of PEO protons. This peak is absent from the corresponding WISE NMR spectrum (Figure 9c) in which only the signals of weakly dipolar-coupled protons are visible. This suggests that the mobility of PEO segments near the clay surface is strongly reduced. After 10 ms of spin diffusion, the magnetization of more distant PEO segments contributes to the HETCOR spectrum (Figure 9f). A fraction of mobile PEO segments is seen in the corresponding 10 ms WISE spectrum (Figure 8d).

The reduced mobility of PEO is also apparent from the ^{1}H wide-line spectra shown in Figure 10. Both with and without MAS, the PS4EO-HCT exhibits a much larger line width. On the basis of the ^{1}H−^{29}Si WISE which proves the proximity of these segments to the silicate surface, this ^{1}H line broadening can safely be attributed to the confinement of PEO in the clay galleries. The narrow PEO signal in Figure 10b,d

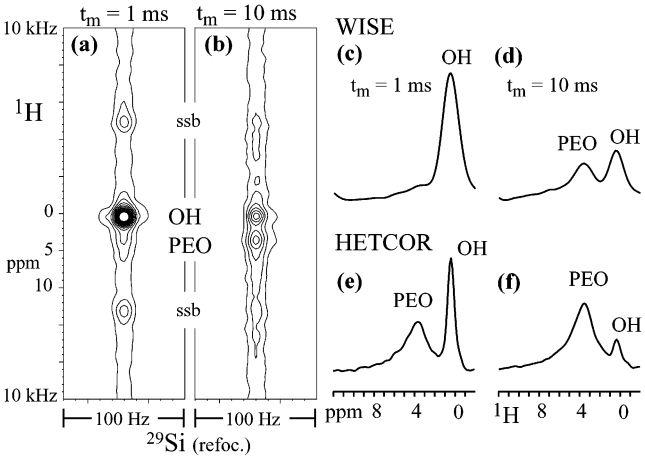

Figure 9. Two-dimensional ^{1}H−^{29}Si WISE NMR spectra with spin diffusion for PS4EO-HCT for spin diffusion times of (a) 1, (b) 10, and 1.5 ms of LGCP. The labels "ssb" mark spinning sidebands. (c, d): Cross sections through the spectra in (a) and (b), respectively, exhibiting only a small signal fraction of mobile PEO. (e, f): For reference, cross sections through 2D ^{1}H−^{29}Si HETCOR NMR spectra at spin diffusion time of 1 and 10 ms, respectively.

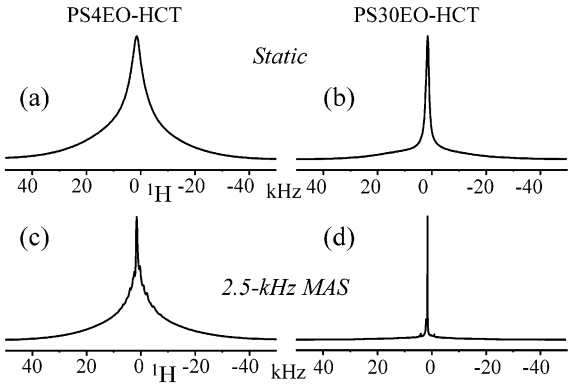

Figure 10. Static ^{1}H wide-line spectra of (a) PS4EO-HCT and (b) PS30EO-HCT. ^{1}H wide-line spectra at 2.5 kHz MAS of (c) PS4EO-HCT and (d) PS30EO-HCT. The increased line width in (a) and (c) relative to (b) and (d) indicates reduced mobility of a large fraction of the PEO segments.

indicates that in PS30EO-HCT a significant fraction of PEO is not confined, being highly mobile.

^{1}H Inversion Recovery. A simple method for assessing ^{1}H spin diffusion on a time scale of several hundred milliseconds is ^{1}H inversion recovery. Differences in ^{1}H T_1 relaxation times reflect incomplete spin diffusion on the time scale of the recovery delay. The data of Figure 11 show different inversion recovery behaviors of the sharp and the broad PEO signals. At 180 ms, the broad PEO and OH signals pass through zero, revealing the signal of the mobile PEO, which has a longer T_1 relaxation time. This means that the magnetization of intercalated and nonintercalated polymer does not equilibrate by spin diffusion on a 200 ms time scale.

^{1}H Spin Diffusion Analysis. Figure 12 shows the spin diffusion curves for the two PSEO-HCT samples, which were obtained by evaluating peak areas in the cross sections of ^{1}H−^{1}H homonuclear correlation (Figure 8a,c) and 2D ^{1}H−^{29}Si HETCOR experiments (Figure 5) with spin diffusion. The *y*-axis displays the area of the clay-OH peak (I_{OH}) normalized by the overall integral intensity of the spectrum. This normalization corrects for the T_1 effect to first order. The square root of the

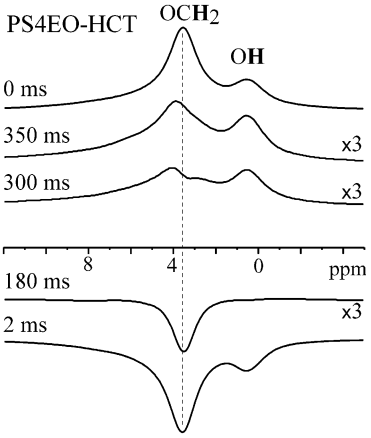

Figure 11. ^{1}H inversion recovery for the PS4EO-HCT sample, showing that on the 200 ms time scale spin diffusion does not equilibrate the magnetization between the intercalated PEO (broad signal, in equilibrium with OH) and the mobile PEO (narrow line with longer T_1 relaxation time, observed selectively at 180 ms recovery time).

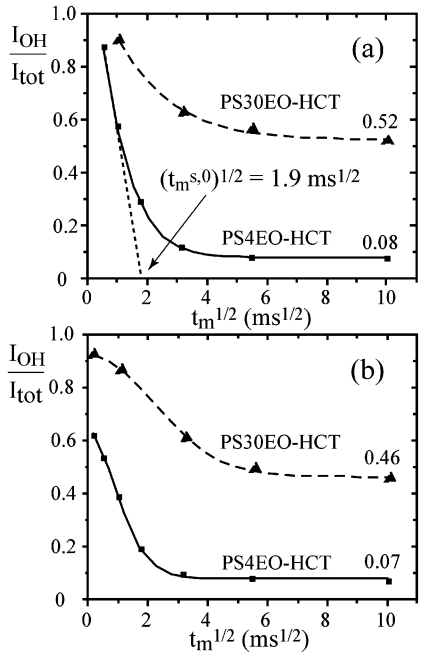

Figure 12. (a) Spin diffusion diagram obtained from the ^{1}H−^{1}H correlation data of Figure 7 and (b) from the ^{1}H−^{29}Si HETCOR data of Figure 4 with spin diffusion, for both PS-EO-HCT samples. The normalized integral OH-proton intensity, $I_{OH}/(I_{OH} + I_{PEO})$, has been plotted against the square root of the mixing time. The curves are guides to the eye.

mixing time ($\sqrt{t_m}$) is the *x*-coordinate. In Figure 12b, the initial relative intensity of clay-OH for PS4EO-HCT is reduced to ca. 0.6 already at very short mixing time (3 μs) as a result of fast heteronuclear magnetization transfer from PEO protons to ^{29}Si during ^{1}H−^{29}Si Lee−Goldburg cross-polarization.[23]

At short spin diffusion times, the magnetization transfer from clay-OH protons to PEO in PS4EO-HCT will be along the direction perpendicular to the silicate layer; this process is very fast because the thickness of the polymer layer between the silicate surfaces is only ~1 nm. By the extension of the initial linear slope, the value $\sqrt{t_m^{s,0}}$ is obtained as the intercept with the *X*-axis (see Figure 12a). The diffusion length can thus be estimated from the initial rate approximation.[21,24] Using the formula given in ref 21 and assuming a spin

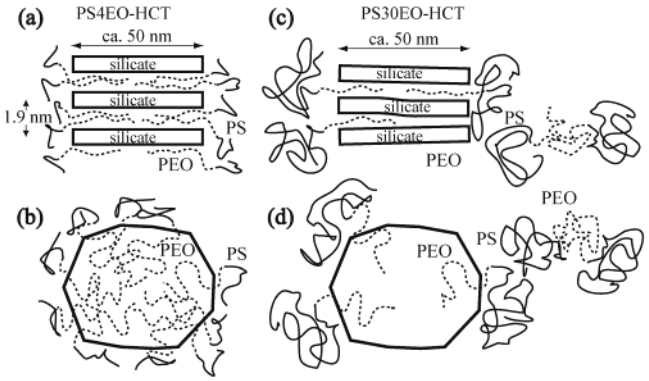

Figure 13. Schematic structural models of the PS-EO-HCT samples, obtained from NMR and X-ray data. PEO blocks are shown as dashed lines and PS blocks as solid lines. The outlines of the clay platelets are indicated by thick lines. (a) PS4EO-HCT, side view. The plate thickness and interlayer gap are magnified in order to make the intercalated polymer segments visible. (b) PS4EO-HCT, top view. For clarity, only a few of the intercalated polymer chains are sketched. (c) PS30EO-HCT, side view. The limited amount of PEO available for intercalation results in stacking disorder. On the basis of the NMR results, a significant PEO fraction is shown as not intercalated. (d) PS30EO-HCT, top view.

diffusion coefficient of 0.4 nm^2/ms for the intercalated, less mobile PEO protons, the spin diffusion length between the clay-OH protons and the intercalated PEO protons is estimated to be ca. 1.4 nm. This is probably an overestimate due to the low proton density in the silicate, which slows down spin diffusion. By comparison, the spin diffusion in PS30EO-HCT is seen to be much slower and involves a much smaller fraction of the OH-proton magnetization.

Structural Models of PS-*b*-PEO Composites with Clay. On the basis of the information obtained from the spin diffusion NMR and WAXD data, we propose a structural model for the PS-*b*-PEO sample with intercalated PEO block (PS4EO-HCT) (see Figure 13a,b). The typical plate diameter (layer length) of hectorite clay is about 50 nm.[2] The length of the PEO block is comparable. The contour length in the stretched-out all-trans conformation is 60 nm. More realistically, we should consider that, in the helical structure of a PEO chain in the crystalline state, seven $-OCH_2CH_2$ units constitute the fiber identity period of 1.93 nm. The extended-helix length of PEO blocks in the PS4EO molecules would thus be ca. 44 nm, i.e., more than the 25 nm radius of the clay platelets. The result of the $^1H-^1H$ correlation experiment indicates that a $\geq$5 nm length of PEO block is not intercalated; thus, at least 80% the length of the PEO block in the PS4EO molecules extends into the clay stack. The PS block and at least 10% of the PEO block are outside the clay, as a surface layer around the clay stacks.

For the PS30EO block copolymer, despite the slightly greater length of the PEO blocks (ca. 53 nm extended helix length), the amount of intercalated PEO is much smaller, according to the NMR data. A model that is consistent with both NMR and WAXD data is sketched in Figure 13c,d. It is characterized by incomplete PEO intercalation and resulting stacking disorder. The WAXD peak position suggests that PEO is intercalated as a single layer, but it should be noted that a dense PEO layer is quite unlikely given the NMR results. The (001) WAXD peak position is usually taken as a measure of a specific long period of the stacked clay system, but it has been shown that silicate volume fractions, experimental conditions, and disorder of the second kind[25] in the layer stacking will also affect the basal reflection. Vaia has shown[26] that disorder of the second kind not only broadens the (001) peak but also shifts it to lower 2θ angles even if the mean layer spacing is unchanged (see Figure 12 of ref 26). Silicate stacking disorder of this nature would be the likely result of partial intercalation of a small amount of PEO into the clay tactoids, as illustrated in Figure 13c,d.

The reason for the limited intercalation of PEO must be sought in the 8 times greater length of the PS block compared to that in the PS4EO copolymer. First of all, the amount of PEO in the PS30EO-HCT sample is 3 times smaller than in the PS4EO-HCT material. Thus, not enough PEO is available for full-coverage intercalation. In addition, there will be a major mismatch of cross-section area at the interface between an intercalated PEO block and a PS Gaussian coil, unless the PS coil is highly elongated, which may result in a high free energy penalty. In other words, the "mushroom cap" formed by a PS coil will block other chains from intercalating from the same region along the rim of the clay stack (see Figure 13c). The narrow PEO signal in Figure 10b,d indicates that in PS30EO-HCT a significant fraction of PEO is not confined, being highly mobile. This requires us to place some PEO blocks outside the clay layers (see Figure 13c,d). Overall, the details of the model of PS30EO-HCT are less certain than those of the model of PS4EO-HCT.

Conclusions

We have determined the extent of intercalation of PS-*b*-PEO copolymers in hectorite clay by using two-dimensional $^1H-^{29}Si$, $^1H-^1H$, and $^1H-^{13}C$ correlation experiments with ^1H spin diffusion. We have shown that in PS4EO-HCT at least 80% of the 7 kDa PEO block is intercalated into the silicate galleries. The mobility of the intercalated PEO segments is found to be strongly reduced. The PEO block does not pull the 3.6 kDa PS block into the silicate galleries. In the PS30EO-HCT sample, which has a much longer 30 kDa PS block and therefore a lower PEO fraction, the amount of intercalated PEO is small, and a significant fraction of the PEO is not intercalated.

Acknowledgment. The authors thank Dr. R. A. Vaia for helpful comments. This work was supported by the Director for Energy Research, Office of Basic Energy Science, in the Materials Chemistry Program of Ames Laboratory, operated for the U.S. Department of Energy by Iowa State University (Contract W-7405-Eng-82). T.J.B. thanks the Fundação de Amparo à Pesquisa do Estado de São Paulo (FAPESP)-Brazil for a fellowship.

References and Notes

(1) Giannelis, E. P.; Krishnamoorti, R.; Manias, E. *Adv. Polym. Sci.* **1999**, *138*, 107.
(2) Alexandre, M.; Dubois, P. *Mater. Sci. Eng., R* **2000**, *28*, 1.
(3) Biswas, M.; Ray, S. S. *Adv. Polym. Sci.* **2001**, *155*, 167.
(4) Pinnavaia, T. J.; Beall, G. W. E. *Polymer-Clay Nanocomposite*; Wiley Series in Polymer Science; Wiley: Chichester, England, 2000.
(5) Vaia, R. A.; Vasudevan, S.; Krawiec, W.; Scanlon, L. G.; Giannelis, E. P. *Adv. Mater.* **1995**, *7*, 154.
(6) Vaia, R. A.; Sauer, B. B.; Tse, O. K.; Giannelis, E. P. *J. Polym. Sci., Part B: Polym. Phys.* **1997**, *35*, 59.

(7) Harris, D. J.; Bonagamba, T. J.; Schmidt-Rohr, K. *Macromolecules* **1999**, *32*, 6718.
(8) Fisher, H. R.; Gielgens, L. H.; Koster, T. P. M. *Acta Polym.* **1999**, *50*, 122.
(9) Morgan, A. B.; Gilman, J. W. *J. Appl. Polym. Sci.* **2003**, *87*, 1329.
(10) Schmidt-Rohr, K.; Spiess, H. W. *Multidimensional Solid-State NMR and Polymers*, 1st ed.; Academic Press: San Diego, CA, 1994.
(11) Ying, D.-K.; Zax, D. B. *J. Chem. Phys.* **1999**, *110*, 5325.
(12) Kwiatkowski, J.; Whittaker, A. K. *J. Polym. Sci., Part B: Polym. Phys.* **2001**, *39*, 1678.
(13) Gougeon, R. D.; Reinholdt, M.; Delmotte, L.; Miehe-Brendle, J.; Chezeau, J.-M.; Dred, R. L.; Marchal, R.; Jeandet, P. *Langmuir* **2002**, *18*, 3396.
(14) Hou, S.-S.; Beyer, F. L.; Schmidt-Rohr, K. *Solid State Nucl. Magn. Reson.* **2002**, *22*, 110.
(15) Bennett, A. E.; Rienstra, C. M.; Auger, M.; Lakshmi, K. V.; Griffin, R. G. *J. Chem. Phys.* **1995**, *103*, 6951.
(16) Young, S. K.; Jarrett, W. L.; Mauritz, K. A. *Polymer* **2002**, *43*, 2311.
(17) Alba, M. D.; Becerro, A. I.; Castro, M. A.; Perdigon, A. *Chem. Commun.* **2000**, 37.
(18) Engelhardt, G.; Michel, D. *High-Resolution Solid-State NMR of Silicates and Zeolites*; Wiley: New York, 1987.
(19) Carrado, K. A.; Xu, L.; Gregory, D. M.; Song, K.; Seifert, S.; Botto, R. E. *Chem. Mater.* **2000**, *12*, 3052.
(20) Gerstein, B. C.; Chow, C.; Pembleton, R. G.; Wilson, R. C. *J. Chem. Phys.* **1977**, *81*, 565.
(21) Mellinger, F.; Wilhelm, M.; Spiess, H. W. *Macromolecules* **1999**, *32*, 4686.
(22) Schmidt-Rohr, K.; Clauss, J.; Spiess, H. W. *Macromolecules* **1992**, *25*, 3273.
(23) Lee, M.; Goldburg, W. I. *Phys. Rev.* **1965**, *140*, A1261.
(24) Clauss, J.; Schmidt-Rohr, K.; Spiess, H. W. *Acta Polym.* **1993**, *44*, 1.
(25) Roe, R.-J. *Methods of X-ray and Neutron Scattering in Polymer Science*; New York, 2000.
(26) Pinnavaia, T. J.; Beall, G. W. *Polymer-Clay Nanocomposite*; Wiley Series in Polymer Science; Wiley: Chichester, England, 2000, Chapter 12, p 248.

MA025707F